Eur. Phys. J. D **9**, 647–651 (1999)

**THE EUROPEAN PHYSICAL JOURNAL D**
EDP Sciences
© Società Italiana di Fisica
Springer-Verlag 1999

# Greengold, a giant cluster compound of unusual electronic structure

E. Gutiérrez[1], R.D. Powell[1], F.R. Furuya[1], J.F. Hainfeld[1,2], T.G. Schaaff[3], M.N. Shafigullin[3], P.W. Stephens[4], and R.L. Whetten[3]

[1] Nanoprobes Inc., Stony Brook, NY 11790-3350, USA
[2] Biology Division, Brookhaven National Laboratory, Upton, NY 11794, USA
[3] School of Physics and Chemistry, Georgia Institute of Technology, Atlanta, GA 30332-0430, USA
[4] Department of Physics, State University of New York, Stony Brook, NY 11794, USA

Received: 1 September 1998 / Received in final form: 20 March 1999

**Abstract.** We report the isolation of a previously elusive giant gold-cluster compound with unusual electronic structure and excellent solid-state ordering properties. *Greengold* is a water-soluble Au:PR$_3$ compound (R= $p$-C$_6$H$_4$−CONHCH$_3$) formed in high yield in the solution-phase reduction of R$_3$PAuCl. Following chromatographic isolation, it has been investigated by electron microscopy (STEM), optical spectroscopy, mass spectrometry (MALDI), and X-ray diffraction, from which emerges a consistent picture of Greengold's intrinsic characteristics as (i) a single compound of ∼22 000 amu molecular weight, containing a strongly bound globular metal core of mass 14 800 (Au$_{75}$, 1.3-nm equivalent diameter); (ii) a highly ordered solid, exhibiting diffraction through 21 orders of a 2.47-nm spacing; and (iii) a carrier of a highly structured optical absorption across the entire visible and near-infrared spectrum (to ∼1.0 eV), including relative transparency in the blue and yellow regions, giving rise to its eponymous green tint.

**PACS.** 61.46.+w Clusters, nanoparticles, and nanocrystalline materials

Lying beyond the well established large gold-cluster compounds (e.g. those based on Au$_{11}$ or Au$_{13}$) [1], there is a series of giant compounds [2–4] whose rigorous isolation and characterization have faced grave difficulties even as they have sustained great fundamental interest [5, 6] and an expanding applications market as bioconjugate probes [7], in addition to other possible applications [8]. One of these, a Au$_{39}$(PR$_3$)$_{14}$Cl$_8$ compound with an *hcp*-derived metal core [4], has undergone a complete structural characterization, but its other properties remain inaccessible. Still larger compounds of the same family have not yielded to definite structure-composition determination, yet have been extensively investigated for their physical and chemical properties [5, 8, 9] while their precise identities remain a matter of debate [10, 11]. More recently, a series of giant Au:SR cluster compounds [12, 13], analogous to the popular extended surface phases (self-assembled monolayers) [14], has been identified and found to possess interesting metal-derived spectroscopic and electrochemical properties [15].

One difficulty associated with the classic Au:PR$_3$:X system (R = aryl; X = halogen) has been illustrated by a comparative mass-spectrometric investigation [16] of the giant-cluster compounds, prepared in four independent labs, indicating that three distinct compounds may predominate – as mixtures – in the filtered samples with molecular weights (for R = phenyl) near 11 000, 14 000 and 20 000 amu. The first value is near that of the above-mentioned Au$_{39}$ compound, and the second is near that determined (by ultracentrifugation) by Schmid *et al.* [3] There is an evident need for a complete separation of these and any other species prior to drawing any final conclusion about their structural and electronic properties.

The commercial Nanogold® product [7] consists of one or more members of this Au:PR$_3$ family (R = $p$-C$_6$H$_4$−CONHCH$_3$) that have been chromatographically separated from the much lighter Undecagold compound Au$_{11}$, as well as from any much larger (colloidal) gold species. In the STEM, the average core-diameter is ∼1.4 nm, but slight variations in size are apparent. Recently, one of us (EG) found that a modified size-exclusion chromatography (see appendix) could indeed separate (Fig. 1a) not only the orange-tinted Undecagold, but also two fractions from the previously unresolved Nanogold® peak, one of brownish and the other of greenish (hence Greengold) color. In the STEM, this new Greengold compound (Fig. 2) shows a very high uniformity of scattering centers (cluster Au cores), and good short-range ordering. Figure 1b compares the optical spectra of Undecagold, Greengold, and the unseparated Nanogold® mixture. The falling extinction coefficient for the smaller Undecagold compound at 2.1 eV is consistent with the orange color seen in the last band eluted from the column separation. The color of Greengold arises from the minima in optical extinction in the yellow (2.2 eV) and blue (2.7 eV) regions of the spectrum. Finally, the optical spectrum of the Nanogold®

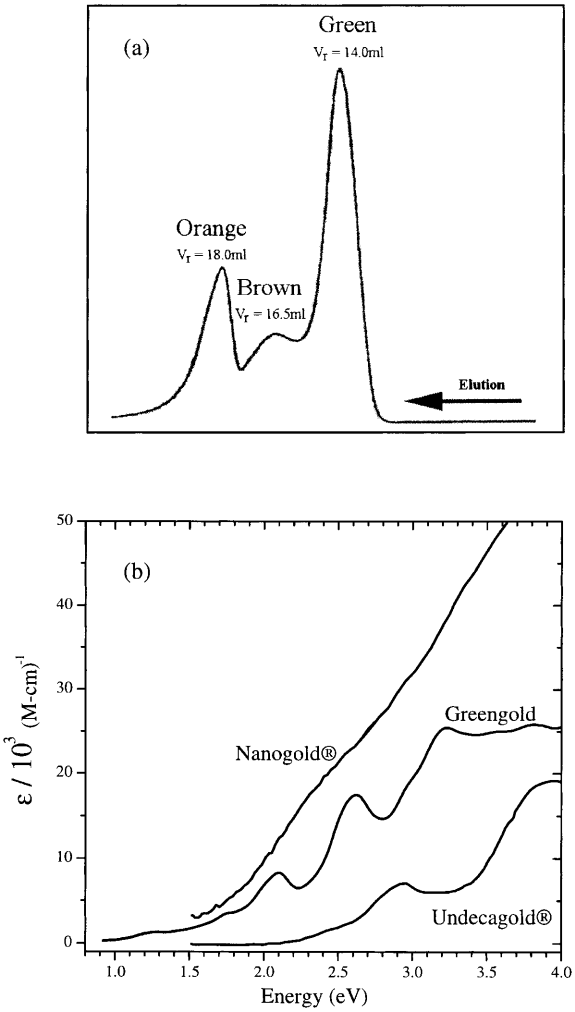

**Fig. 1.** (a) Chromatogram illustrating the separation of the large gold cluster compounds identified as Brown- and Greengold. (b) Comparison of the optical spectra of the Undecagold, the highly abundant Greengold, and the Nanogold® mixture. For Undecagold and Greengold the absolute extinction is shown; however, Nanogold® sample extinction was scaled arbitrarily.

mixture agrees with that of Schmid's "$\mathrm{Au}_{55}$" compound in that it "appears rather structureless, neither showing a collective excitation resonance nor exhibiting distinct absorption bands as for lower nuclearity clusters" [17].

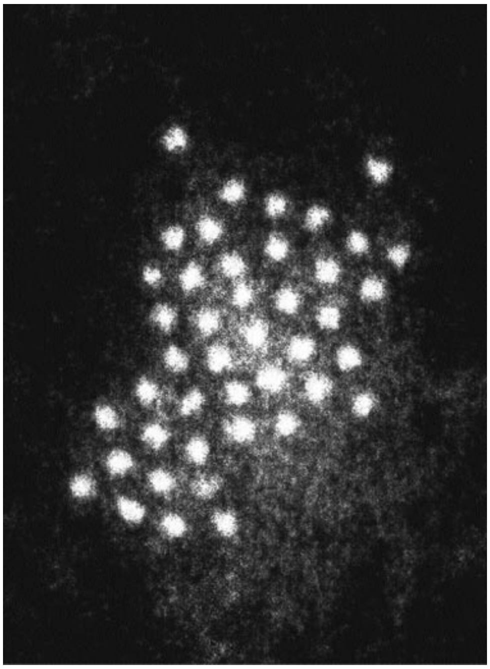

**Fig. 2.** STEM image showing exceptional uniformity and brilliance (contrast) of the cluster cores from the Greengold compound. The mean core diameter is 1.3 nm.

The negative-ion mass spectra of the Greengold sample (Fig. 3) were obtained through the matrix-assisted laser desorption ionization time-of-flight (MALDI-TOF) studies from both poorly and well co-crystallized samples. When desorbing ions from poorly co-crystallized films (analyte concentrated at the film surface), extensive fragmentation can occur, leaving a pattern of ion intensities consistent with the complete removal of all ligands, so that only $[\mathrm{Au}_N]^-$ clusters remain (Fig. 3a). The peaks shown in the inset of the Fig. 3a correspond to ions with $N = 68$ to 73, with a weaker, poorly resolved tail extending to $\mathrm{Au}_{75}$. In the case of well co-crystallized films (low analyte concentration), the desorbed ions are measured at a considerably higher mass centered at ~21 kDa (Fig. 3b), with a sharp intensity drop (arrow) just above ~21.7 kDa, which could correspond to the total molecular weight of the intact cluster compound. The overall breadth and shape of this 21 kDa band are consistent with a partial loss of the ligand shell, but the instrumental resolution did not allow identification of individual ions. Thus, the combination of the two spectra gives clear evidence for a strongly bound Au core of 73-75 atoms, and a fragile parent ion with the molecular weight of 21.7 kDa, or slightly higher. This estimated molecular weight is shifted from the 20 kDa feature identified earlier [16] by the amount consistent with the additional mass of the aryl derivatization ($-\mathrm{CONHCH}_3$). The equivalent diameter of an $\mathrm{Au}_{73-75}$ core, calculated assuming the density of bulk gold (60 atoms/nm$^3$), is 1.33 nm, consistent with the STEM results and the X-ray diffraction studies, to be described next.

Evaporation of an aqueous solution on a silicon wafer yields an optically thin film with exceptional crystallographic order, as seen in the intense X-ray diffraction pattern (Fig. 4, solid phase), obtained in reflection geometry. The diffraction pattern is dominated by a long series of reflections, through the 21st order, corresponding to a single lattice-plane spacing of 2.473 nm. By contrast, known giant gold cluster compounds of this family, beyond $\mathrm{Au}_{39}$, exhibit no proper Bragg diffraction [10,18]. Variations in the observed solid-phase peak intensities with increasing values of s are consistent with oscillations in the form factor of individual nanocrystals (Fig. 4, dashed line). The apparent revival in the region from 4.0 to 5.3 nm$^{-1}$ encompasses the (111) and (200) reflections of bulk gold, which is consistent with scattering due to close-packing of Au

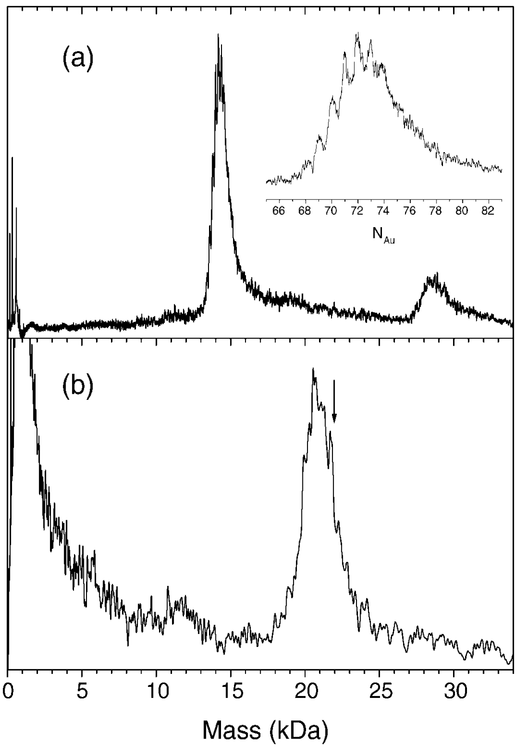

**Fig. 3.** The negative-ion MALDI mass spectra for Greengold under poor (a) and well (b) co-crystallized conditions [26]. The inset (a) shows an expanded view of the main band, plotted in Au-atom units. The arrow in (b) marks the tentative assignment of the total molecular weight.

atoms within individual clusters, as seen in the solution-phase diffraction pattern (dashed line). The envelope of the peak intensities in that region has a width (FWHM) of $\Delta s \sim 0.7\,\mathrm{nm}^{-1}$, as expected for a 1.3 nm diameter crystallite. Highly ordered extended arrays , or thin molecular crystals can also be imaged directly with STEM (Fig. 5). Long-range close-packing seen in this image correlates well with the diffraction data, and serves as yet another confirmation of the exceptional uniformity of the sample.

The consistent picture of Greengold that emerges from these independent measurements is obvious from the structural and compositional information above. The high degree of order and simplicity of the XRD, STEM, and MS analyses points to the presence of a single, well defined compound. From the MS background, any minor (impurity) species are estimated to be present below the 5% level. Similarly, the optical absorption spectrum is highly distinctive and unlikely to arise from a mixture. Plausible Au-core structures in the 73-75 atom range have been described recently by Cleveland *et al.* [19] With $PR_3$ (433 amu) contributions one arrives at a plausible composition in the range of $Au_{73-75}(PR_3)_{15-17}Cl_x$.

In stark contrast to previous reports [17, 20, 21] on giant gold-phosphine cluster compounds (or mixtures), many bands of Greengold's optical spectrum indicate a highly non-continuum electronic structure. Figure 6 presents the spectral function replotted so as to emphasize the near-infrared region (0.8 to 1.6 eV), along with a diagram proposing interpretation in terms of the band-structure of bulk gold and gold clusters [22, 23]. Within this picture, the weak bands and shoulders (a-d) appearing below 2.0 eV arise from discrete *intra*band transitions within the 6*sp* conduction band, whereas the stronger and broader bands in the visible and near-ultraviolet region (2.0 to 4.0 eV) arise from *inter*band transitions $5d \rightarrow 6sp$, i.e. originating in the submerged and quasicontinuum 5*d*-band and terminating in the lowest unoccupied conduction-band levels. The average density of levels is roughly similar to that obtained in first principles calculations on a hypothetical $I_h$-$Au_{55}$ cluster [22]. (The same diagram has been used to explain the band structure in the large and giant Au:SR cluster compounds [24]). An absorption edge, or onset, just below 1.0 eV could indicate a large HOMO-LUMO gap, consistent with the preferential accumulation and high stability of this favored cluster compound.

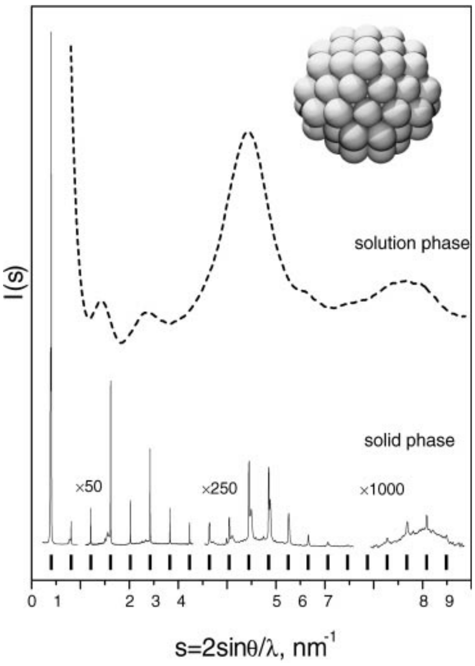

**Fig. 4.** X-ray diffraction patterns obtained from film (solid line) and solution (dashed line) samples of Greengold. The film shows reflections through the 21st order (bars), with the peak intensity variations consistent with the solution-phase data. The 75-atom structural model (inset) is discussed in [19].

In the case of the $Au_{11}^{3+}$ Undecagold compound, the eight-electron $S^2P^6$ valence configuration can account for its high sphericity, stability, abundance and molecule-like electronic structure [25]. For Greengold, both structural and electronic arguments could be invoked to account for its formation and other properties: First, the 75-atom truncated-decahedral structure (Fig. 4, inset) has been identified as having superior energetic stability [19]. Second, the electronic shell closings at 68 or 70 electrons would be relevant, depending on the cluster charge (i.e. the number of halide ions associated with the structure.) These questions will be resolved by continuing structural, compositional and electronic investigations into this remarkable new compound.

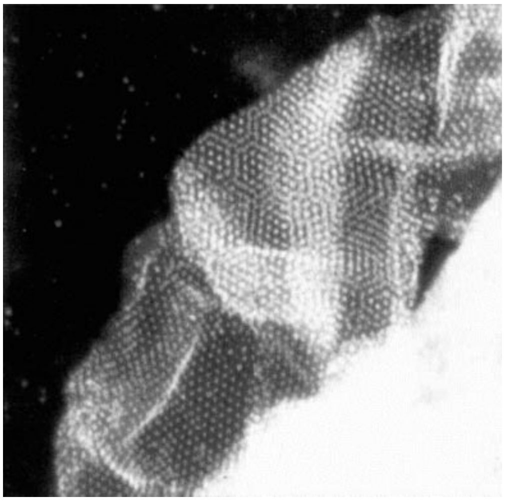

**Fig. 5.** Low-resolution STEM image showing exceptional long-range ordering observed in a sample of Greengold. Single Au-cluster cores are visible in the upper left. Patterns consistent with ordered bi- and tri-layer films dominate the central region.

We would like to thank Dr. Joseph Khoury, Prof. Lauren Tolbert, and Prof. Angus Wilkinson. Research at Nanoprobes has been supported by NIH Small Business Innovation Research Grants (R44 GM 49564) and (R44 GM 50048) and research at Georgia Institute of Technology has been supported by NSF (CHE-9700562).

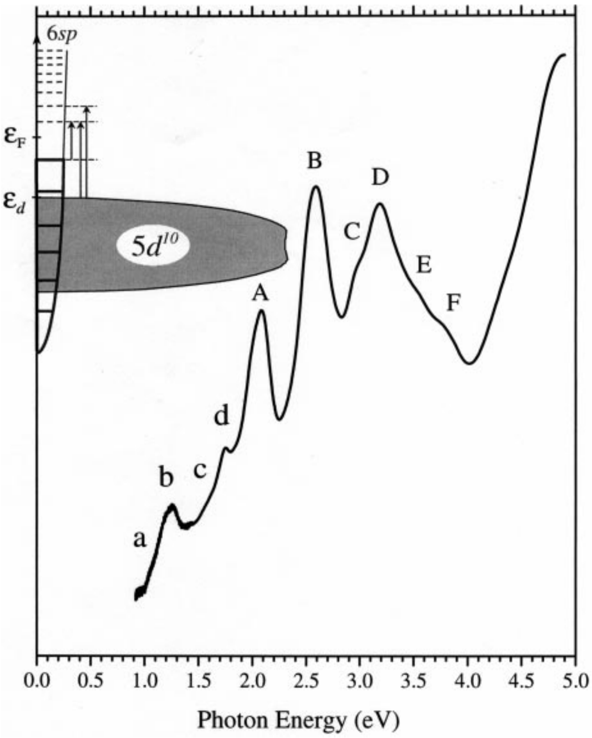

**Fig. 6.** The optical absorption spectrum for Greengold, multiplied by $\omega^{-2}$. Inset: idealized band structure of bulk *fcc*-Au cluster, with discrete levels and transitions (arrows) to account for finite-size effects. The *inter*band energy difference $\varepsilon_F - \varepsilon_d = 1.7\,\text{eV}$.

## Appendix: Methods

**Preparation and isolation of Greengold.** The synthesis involves controlled production of a mixture containing predominantly Greengold via Au(I) starting materials, a specialized tri-aryl phosphine and borane or borohydride as base in dimethylacetamide (DMA) [7]. Good separation of the resulting mixture of cluster sizes is achieved in 20 mM phosphate, 150 mM NaCl, pH = 7.4 using a Superose 12 (Pharmacia Biotech) column, at a flow rate of 0.4 mL/min, 1 mL loading.

**Mass spectrometry.** Mass spectra were generated by a custom-made reflectron-type time-of-flight mass spectrometer, using the third harmonic (355 nm) of a Q-switched Nd:YAG laser (Continuum). The negative ions are accelerated to −5 kV into a field-free region, reflected from an electrostatic mirror and detected by a conversion-dynode/microchannel plate system. Flight times are calibrated against protein standards using precisely the same target matrix, laser fluence and other mass spectrometer parameters. The matrix samples are prepared (co-crystallized) from a 0.07 M 2,4-dihydroxybenzoic acid and $3 \times 10^{-5}$ to $1 \times 10^{-4}$ M analyte (cluster compound) solution. Mass spectra are typically accumulated over 20–50 consecutive laser pulses. The spectra obtained from the initial irradiation of a freshly prepared sample are very strong (high intensity), show aggregation peaks, and give extensive fragmentation, indicating poor co-crystallization of the analyte at the surface [26]. Continued irradiation evaporates such regions, allowing a proper MALDI effect to be obtained, characterized by much weaker signal intensity, reduced aggregation, and a great reduction in fragmentation.

**X-ray diffraction.** Both solid- and solution-phase diffraction patterns were obtained at the National Synchrotron Light Source, using monochromatized synchrotron X-ray radiation ($\lambda = 1.11501$ A). Solid-phase XRD pattern was measured in the reflection mode from a thin film prepared by depositing an aqueous solution on a miscut $\text{Si}_{111}$ wafer and air-drying. Solution-phase data were obtained from a concentrated MeOH solution of Greengold in a 1.0 mm glass capillary. Experimental diffractograms have been corrected for background, absorption, polarization and geometry-dependent parameters.

## References

1. D.M.P. Mingos: J. Chem. Soc. Dalton Trans. 561 (1997)
2. G. Schmid: Inorg. Synth. **27**, 214 (1990)
3. G. Schmid, R. Pfeil, R. Boese, T. Bandermann, S. Meyer, G.H.M. Calis, J.W.A. van-der-Velden: Chem. Ber. 3634 (1981)
4. B.K. Teo, X. Shi, H. Zhang: J. Am. Chem. Soc. **113**, 2743 (1992)

5. R.C. Theil, R.E. Benfield, R. Zanoni, H.H.A. Smit, M.W. Dirkin: Struct. Bond. **81**, 1 (1993)
6. G. Schön, U. Simon: Colloid Polym. Sci. **273**, 202 (1995)
7. J.F. Hainfeld, F.R. Furuya: J. Histochem. Cytochem. **40**, 177 (1992)
8. G. Schmid: Chem. Rev. **92**, 1709 (1992)
9. D. Fenske, G. Longoni, G. Schmid: in *Clusters and colloids: from theory to applications*, ed. by G. Schmid (VCH, Weinheim 1994)
10. W. Vogel, B. Rosner, B. Tesche: J. Phys. Chem. **97**, 11 611 (1993)
11. H. Weller: Adv. Mater. **7**, 94 (1995)
12. M.M. Alvarez, J.T. Khoury, T.G. Schaaff, M.N. Shafigullin, I. Vezmar, R.L. Whetten: Chem. Phys. Lett. **266**, 91 (1997)
13. T.G. Schaaff, M.N. Shafigullin, J.T. Khoury, I. Vezmar, R.L. Whetten, W.G. Cullen, P.N. First, C. Gutiérrez, J. Ascensio, M.J. Jose-Yacamán: J. Phys. Chem. B **101**, 7885 (1997)
14. E. Delamarche, B. Michel, H.A. Biebuyck, C. Gerber: Adv. Mater. **8**, 719 (1996)
15. S. Chen, R.S. Ingram, M.J. Hostetler, J.J. Pietron, R.W. Murray, T.G. Schaaff, J.T. Khoury, M.M. Alvarez, R.L. Whetten: Science **280**, 2098 (1998)
16. C.J. McNeal, R.E.P. Winpenny, J.M. Hughes, R.D. MacFarlane, L.H. Pignolet, L.T.J. Nelson, T.G. Gardner, L.H. Irgens, G. Vigh, J.J.P. Fackler: Inorg. Chem. **32**, 5582 (1993)
17. K. Fauth, U. Kreibig, G. Schmid: Z. Phys. D **20**, 297 (1991)
18. D.H. Rapoport, W. Vogel, H. Colfen, R. Schlögl: J. Phys. Chem. **101**, 4175 (1997)
19. C.L. Cleveland, U. Landman, T.G. Schaaff, M.N. Shafigullin, P.W. Stephens, R.L. Whetten: Phys. Rev. Lett. **79**, 1873 (1997)
20. K. Fauth, U. Kreibig, G. Schmid: Z. Phys. D **12**, 515 (1989)
21. D.G. Duff, A. Baiker, P.P. Edwards: J. Chem. Soc. Chem. Commun. 96 (1993)
22. O.D. Häberlen, S.C. Chung, M. Stener, N.R. Rösch: Ber. Bunsenges. Phys. Chem. **106**, 5189 (1997)
23. K.J. Taylor, C.L. Pettiette-Hall, O. Cheshnovsky, R.E. Smalley: J. Chem. Phys. **96**, 3319 (1992)
24. M.M. Alvarez, J.T. Khoury, T.G. Schaaff, M.N. Shafigullin, I. Vezmar, R.L. Whetten: J. Phys. Chem. B **101**, 3706 (1997)
25. D.M.P. Mingos: Chem. Soc. Rev. **15**, 31 (1986)
26. T.G. Schaaff: Ph.D. Dissertation, Georgia Institute of Technology (1998)